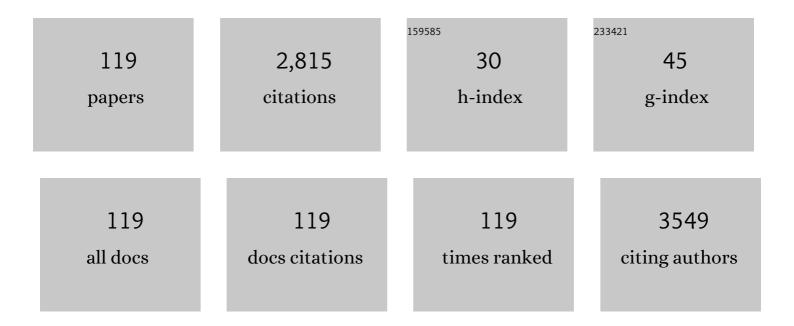
## Roberto Fattorusso

List of Publications by Year in descending order

Source: https://exaly.com/author-pdf/4090301/publications.pdf Version: 2024-02-01



#	Article	IF	CITATIONS
1	Targeting angiogenesis: Structural characterization and biological properties of a de novo engineered VEGF mimicking peptide. Proceedings of the National Academy of Sciences of the United States of America, 2005, 102, 14215-14220.	7.1	242
2	Critical DNA Binding Interactions of the Insulator Protein CTCF. Journal of Biological Chemistry, 2007, 282, 33336-33345.	3.4	139
3	Efficient synthetic inhibitors of anthrax lethal factor. Proceedings of the National Academy of Sciences of the United States of America, 2005, 102, 9499-9504.	7.1	126
4	NMR-based techniques in the hit identification and optimisation processes. Expert Opinion on Therapeutic Targets, 2004, 8, 597-611.	3.4	69
5	The Arabidopsis SUPERMAN protein is able to specifically bind DNA through its single Cys2-His2 zinc finger motif. Nucleic Acids Research, 2002, 30, 4945-4951.	14.5	63
6	The structural role of the zinc ion can be dispensable in prokaryotic zinc-finger domains. Proceedings of the National Academy of Sciences of the United States of America, 2009, 106, 6933-6938.	7.1	54
7	The Inorganic Perspective of Nerve Growth Factor: Interactions of Cu <sup>2+</sup> and Zn <sup>2+</sup> with the Nâ€₹erminus Fragment of Nerve Growth Factor Encompassing the Recognition Domain of the TrkA Receptor. Chemistry - A European Journal, 2011, 17, 3726-3738.	3.3	52
8	The prokaryotic zincâ€finger: structure, function and comparison with the eukaryotic counterpart. FEBS Journal, 2015, 282, 4480-4496.	4.7	51
9	Design, structural and functional characterization of a Temporin-1b analog active against Gram-negative bacteria. Biochimica Et Biophysica Acta - General Subjects, 2013, 1830, 3767-3775.	2.4	50
10	NMR structure of the human oncofoetal fibronectin ED-B domain, a specific marker for angiogenesis. Structure, 1999, 7, 381-390.	3.3	49
11	Neuronal High-Affinity Sodium-Dependent Glutamate Transporters (EAATs): Targets for the Development of Novel Therapeutics Against Neurodegenerative Diseases. Current Pharmaceutical Design, 2003, 9, 599-625.	1.9	47
12	The prokaryotic Cys <sub>2</sub> His <sub>2</sub> zinc-finger adopts a novel fold as revealed by the NMR structure of <i>Agrobacterium tumefaciens</i> Ros DNA-binding domain. Proceedings of the National Academy of Sciences of the United States of America, 2007, 104, 17341-17346.	7.1	47
13	Analysis of a Membrane Interacting Region of Herpes Simplex Virus Type 1 Glycoprotein H. Journal of Biological Chemistry, 2008, 283, 29993-30009.	3.4	47
14	Ubiquitin binds the amyloid $\hat{l}^2$ peptide and interferes with its clearance pathways. Chemical Science, 2019, 10, 2732-2742.	7.4	46
15	A New Ligand for Immunoglobulin G Subdomains by Screening of a Synthetic Peptide Library. ChemBioChem, 2005, 6, 1242-1253.	2.6	44
16	Structural Determinants of the Unusual Helix Stability of a De Novo Engineered Vascular Endothelial Growth Factor (VEGF) Mimicking Peptide. Chemistry - A European Journal, 2008, 14, 4164-4166.	3.3	42
17	Structural Zn(II) Implies a Switch from Fully Cooperative to Partly Downhill Folding in Highly Homologous Proteins. Journal of the American Chemical Society, 2013, 135, 5220-5228.	13.7	41
18	NMR Structure of the Single QALGGH Zinc Finger Domain from the Arabidopsis thaliana SUPERMAN Protein. ChemBioChem, 2003, 4, 171-180.	2.6	40

#	Article	IF	CITATIONS
19	Discovery of a Novel Class of Reversible Non-Peptide Caspase Inhibitors via a Structure-Based Approach. Journal of Medicinal Chemistry, 2005, 48, 1649-1656.	6.4	40
20	Characterization of a Designed Vascular Endothelial Growth Factor Receptor Antagonist Helical Peptide with Antiangiogenic Activity in Vivo. Journal of Medicinal Chemistry, 2011, 54, 1391-1400.	6.4	40
21	Zinc to cadmium replacement in the <i>A. thaliana</i> SUPERMAN Cys <sub>2</sub> His <sub>2</sub> zinc finger induces structural rearrangements of typical DNA base determinant positions. Biopolymers, 2011, 95, 801-810.	2.4	38
22	Zinc to cadmium replacement in the prokaryotic zinc-finger domain. Metallomics, 2014, 6, 96-104.	2.4	37
23	Structural Basis of a Temporin 1b Analogue Antimicrobial Activity against Gram Negative Bacteria Determined by CD and NMR Techniques in Cellular Environment. ACS Chemical Biology, 2015, 10, 965-969.	3.4	37
24	Alpha- and Beta-Cyclodextrin Inclusion Complexes with 5-Fluorouracil: Characterization and Cytotoxic Activity Evaluation. Molecules, 2016, 21, 1644.	3.8	37
25	A Novel Type of Zinc Finger DNA Binding Domain in theAgrobacteriumtumefaciensTranscriptional Regulator Rosâ€. Biochemistry, 2006, 45, 10394-10405.	2.5	34
26	Zinc(II) Complexes of Ubiquitin: Speciation, Affinity and Binding Features. Chemistry - A European Journal, 2011, 17, 11596-11603.	3.3	34
27	Structure and Orientation of the gH625–644 Membrane Interacting Region of Herpes Simplex Virus Type 1 in a Membrane Mimetic System. Biochemistry, 2012, 51, 3121-3128.	2.5	34
28	Neuroblastoma tumorigenesis is regulated through the Nm23-H1/h-Prune C-terminal interaction. Scientific Reports, 2013, 3, 1351.	3.3	34
29	β-Hairpin Peptide That Targets Vascular Endothelial Growth Factor (VEGF) Receptors. Journal of Biological Chemistry, 2011, 286, 41680-41691.	3.4	32
30	Biochemical and Structural Analysis of the Binding Determinants of a Vascular Endothelial Growth Factor Receptor Peptidic Antagonist. Journal of Medicinal Chemistry, 2010, 53, 4428-4440.	6.4	31
31	Traditional Chinese medicines with caspase-inhibitory activity. Phytomedicine, 2006, 13, 16-22.	5.3	29
32	Insights into the anticancer properties of the first antimicrobial peptide from Archaea. Biochimica Et Biophysica Acta - General Subjects, 2017, 1861, 2155-2164.	2.4	29
33	Structural Analysis of a Helical Peptide Unfolding Pathway. Chemistry - A European Journal, 2010, 16, 5400-5407.	3.3	27
34	Zinc(II) Interactions with Brain-Derived Neurotrophic Factor N-Terminal Peptide Fragments: Inorganic Features and Biological Perspectives. Inorganic Chemistry, 2013, 52, 11075-11083.	4.0	27
35	Cationic porphyrins are tunable gatekeepers of the 20S proteasome. Chemical Science, 2016, 7, 1286-1297.	7.4	27
36	The insulin degrading enzyme activates ubiquitin and promotes the formation of K48 and K63 diubiquitin. Chemical Communications, 2015, 51, 15724-15727.	4.1	26

#	Article	IF	CITATIONS
37	A new cryptic host defense peptide identified in human 11-hydroxysteroid dehydrogenase-1 β-like: from in silico identification to experimental evidence. Biochimica Et Biophysica Acta - General Subjects, 2017, 1861, 2342-2353.	2.4	26
38	Genetic and epigenetic mutations affect the DNA binding capability of human ZFP57 in transient neonatal diabetes type 1. FEBS Letters, 2013, 587, 1474-1481.	2.8	25
39	Deciphering the zinc coordination properties of the prokaryotic zinc finger domain: The solution structure characterization of Ros87 H42A functional mutant. Journal of Inorganic Biochemistry, 2014, 131, 30-36.	3.5	25
40	Functional Binding Surface of a βâ€Hairpin VEGF Receptor Targeting Peptide Determined by NMR Spectroscopy in Living Cells. Chemistry - A European Journal, 2015, 21, 91-95.	3.3	25
41	Structural and functional studies of Stf76 from the Sulfolobus islandicus plasmid–virus pSSVx: a novel peculiar member of the winged helix–turn–helix transcription factor family. Nucleic Acids Research, 2014, 42, 5993-6011.	14.5	24
42	Structural and biochemical insights of CypA and AIF interaction. Scientific Reports, 2017, 7, 1138.	3.3	24
43	VEGFR Recognition Interface of a Proangiogenic VEGFâ€Mimetic Peptide Determined In Vitro and in the Presence of Endothelial Cells by NMR Spectroscopy. Chemistry - A European Journal, 2018, 24, 11461-11466.	3.3	24
44	An Experimentally Tested Scenario for the Structural Evolution of Eukaryotic Cys2His2 Zinc Fingers from Eubacterial Ros Homologs. Molecular Biology and Evolution, 2013, 30, 1504-1513.	8.9	23
45	A Combined NMR and Computational Approach to Determine the RGDechiâ€hCitâ€i± <sub>v</sub> î² <sub>3</sub> Integrin Recognition Mode in Isolated Cell Membranes. Chemistry - A European Journal, 2016, 22, 681-693.	3.3	23
46	?-Alanine containing cyclic peptides with turned structure: The?pseudo type II ?-turn.? VI. Biopolymers, 1994, 34, 1517-1526.	2.4	22
47	Solution Structure and Backbone Dynamics of the K18G/R82EAlicyclobacillus acidocaldariusThioredoxin Mutant:à A Molecular Analysis of Its Reduced Thermal Stabilityâ€,‡. Biochemistry, 2004, 43, 6043-6058.	2.5	22
48	VEGFR1 <sub>D2</sub> in drug discovery: Expression and molecular characterization. Biopolymers, 2010, 94, 800-809.	2.4	22
49	Metastatic group 3 medulloblastoma is driven by PRUNE1 targeting NME1–TGF-β–OTX2–SNAIL via PTEN inhibition. Brain, 2018, 141, 1300-1319.	7.6	22
50	Ligand-Based NMR Study of C-X-C Chemokine Receptor Type 4 (CXCR4)–Ligand Interactions on Living Cancer Cells. Journal of Medicinal Chemistry, 2018, 61, 2910-2923.	6.4	22
51	β-Hairpin stabilization through an interstrand triazole bridge. Chemical Communications, 2012, 48, 762-764.	4.1	21
52	Design, structural and biological characterization of a VEGF inhibitor Î <sup>2</sup> -hairpin-constrained peptide. European Journal of Medicinal Chemistry, 2014, 73, 210-216.	5.5	21
53	Miniaturizing VEGF: Peptides mimicking the discontinuous VEGF receptor-binding site modulate the angiogenic response. Scientific Reports, 2016, 6, 31295.	3.3	21
54	Unveiling a VEGF-mimetic peptide sequence in the IQGAP1 protein. Molecular BioSystems, 2017, 13, 1619-1629.	2.9	21

Roberto Fattorusso

#	Article	IF	CITATIONS
55	A crystal structure with features of an antiparallel ?-pleated sheet. Biopolymers, 1994, 34, 1463-1468.	2.4	20
56	?-Alanine containing cyclic peptides with predetermined turned structure. V. Biopolymers, 1994, 34, 1505-1515.	2.4	19
57	Mixed conformation in C?,?-disubstituted tripeptides: X-ray crystal structures of Z-Aib-Dph-Gly-Ome and Bz-Dph-Dph-Gly-Ome. Biopolymers, 1994, 34, 1595-1604.	2.4	18
58	Targeting Zinc Finger Domains with Small Molecules: Solution Structure and Binding Studies of the RanBP2â€Type Zinc Finger of RBM5. ChemBioChem, 2011, 12, 2837-2845.	2.6	18
59	Towards understanding the molecular recognition process in prokaryotic zinc-finger domain. European Journal of Medicinal Chemistry, 2015, 91, 100-108.	5.5	18
60	The (unusual) aspartic acid in the metal coordination sphere of the prokaryotic zinc finger domain. Journal of Inorganic Biochemistry, 2016, 161, 91-98.	3.5	18
61	Folding mechanisms steer the amyloid fibril formation propensity of highly homologous proteins. Chemical Science, 2018, 9, 3290-3298.	7.4	18
62	Molecular strategies to replace the structural metal site in the prokaryotic zinc finger domain. Biochimica Et Biophysica Acta - Proteins and Proteomics, 2014, 1844, 497-504.	2.3	17
63	Ni(II), Hg(II), and Pb(II) Coordination in the Prokaryotic Zinc-Finger Ros87. Inorganic Chemistry, 2019, 58, 1067-1080.	4.0	17
64	Defect peptide chemistry: Perturbations in the structure of a homopentapeptide induced by a guest residue interrupting side-chain regularity. Biopolymers, 1994, 34, 1409-1418.	2.4	16
65	C-terminal truncation of Vascular Endothelial Growth Factor mimetic helical peptide preserves structural and receptor binding properties. Biochemical and Biophysical Research Communications, 2012, 424, 290-294.	2.1	16
66	Structural investigation of the VEGF receptor interaction with a helical antagonist peptide. Journal of Peptide Science, 2013, 19, 214-219.	1.4	16
67	Co(II) Coordination in Prokaryotic Zinc Finger Domains as Revealed by UV-Vis Spectroscopy. Bioinorganic Chemistry and Applications, 2017, 2017, 1-7.	4.1	16
68	MucR binds multiple target sites in the promoter of its own gene and is a heatâ€stable protein: Is MucR a Hâ€ <scp>NS</scp> â€like protein?. FEBS Open Bio, 2018, 8, 711-718.	2.3	15
69	Pyrazolones Activate the Proteasome by Gating Mechanisms and Protect Neuronal Cells from βâ€Amyloid Toxicity. ChemMedChem, 2020, 15, 302-316.	3.2	15
70	Identifying the region responsible for Brucella abortus MucR higher-order oligomer formation and examining its role in gene regulation. Scientific Reports, 2018, 8, 17238.	3.3	14
71	1,2,3â€Triazole Bridge as Conformational Constrain in βâ€Hairpin Peptides: Analysis of Hydrogenâ€Bonded Positions. Chemistry - A European Journal, 2016, 22, 5534-5537.	3.3	13
72	Synthesis and solution characterization of a porphyrin-CCK8 conjugate. Journal of Peptide Science, 2001, 7, 386-394.	1.4	12

**ROBERTO FATTORUSSO** 

#	Article	IF	CITATIONS
73	An NMR and molecular dynamics investigation of the avian prion hexarepeat conformational features in solution. Chemical Physics Letters, 2007, 442, 110-118.	2.6	12
74	NMR assignments of the DNA binding domain of Ml4 protein from Mesorhizobium loti. Biomolecular NMR Assignments, 2010, 4, 55-57.	0.8	12
75	Mapping Functional Interaction Sites of Human Prune Câ€Terminal Domain by NMR Spectroscopy in Human Cell Lysates. Chemistry - A European Journal, 2013, 19, 12217-12220.	3.3	12
76	Structural Insight of the Full-Length Ros Protein: A Prototype of the Prokaryotic Zinc-Finger Family. Scientific Reports, 2020, 10, 9283.	3.3	11
77	Design of metal ion binding peptides. Biopolymers, 1995, 37, 401-410.	2.4	10
78	NMR backbone dynamics studies of human PED/PEAâ€15 outline protein functional sites. FEBS Journal, 2010, 277, 4229-4240.	4.7	10
79	Molecular basis of the PED/PEA15 interaction with the C-terminal fragment of phospholipase D1 revealed by NMR spectroscopy. Biochimica Et Biophysica Acta - Proteins and Proteomics, 2013, 1834, 1572-1580.	2.3	10
80	Long range Trp-Trp interaction initiates the folding pathway of a pro-angiogenic β-hairpin peptide. Scientific Reports, 2015, 5, 16651.	3.3	10
81	Nociceptin reduces the inflammatory immune microenvironment in a conventional murine model of airway hyperresponsiveness. Clinical and Experimental Allergy, 2017, 47, 208-216.	2.9	10
82	12. Zinc Fingers. , 2020, 20, 415-436.		10
83	Determination of the Dihedral Angle Ï <sup>^</sup> Based onJCoupling Measurements in15N/13C-Labeled Proteins. Journal of the American Chemical Society, 1998, 120, 6824-6825.	13.7	8
84	Conformational Features of Human Melanin-Concentrating Hormone: An NMR and Computational Analysis. ChemBioChem, 2003, 4, 73-81.	2.6	8
85	The preferred solidâ€state conformation of (αMe)Trp peptides. International Journal of Peptide and Protein Research, 1995, 45, 70-77.	0.1	8
86	Conformational stabilization of a β-hairpin through a triazole–tryptophan interaction. Organic and Biomolecular Chemistry, 2018, 16, 787-795.	2.8	8
87	Binding mode of AIF(370–394) peptide to CypA: insights from NMR, label-free and molecular docking studies. Biochemical Journal, 2018, 475, 2377-2393.	3.7	8
88	Substitution of the Native Zn(II) with Cd(II), Co(II) and Ni(II) Changes the Downhill Unfolding Mechanism of Ros87 to a Completely Different Scenario. International Journal of Molecular Sciences, 2020, 21, 8285.	4.1	8
89	Synthesis, conformational analysis and immunological activity of β <sup>3</sup> Pheâ€substituted Cyclolinopeptide A analogues. Journal of Peptide Science, 2009, 15, 166-174.	1.4	7
90	Probing the Residual Structure in Avian Prion Hexarepeats by CD, NMR and MD Techniques. Molecules, 2013, 18, 11467-11484.	3.8	7

**ROBERTO FATTORUSSO** 

#	Article	IF	CITATIONS
91	FRET-Protease-Coupled Peptidyl-Prolyl cis-trans Isomerase Assay. Journal of Biomolecular Screening, 2016, 21, 701-712.	2.6	7
92	Deciphering RGDechi peptideâ€Î± 5 β 1 integrin interaction mode in isolated cell membranes. Peptide Science, 2018, 110, e24065.	1.8	7
93	Conformational studies of RGDechi peptide by naturalâ€abundance NMR spectroscopy. Journal of Peptide Science, 2019, 25, e3166.	1.4	7
94	Cooperative Binding of the Cationic Porphyrin Tris-T4 Enhances Catalytic Activity of 20S Proteasome Unveiling a Complex Distribution of Functional States. International Journal of Molecular Sciences, 2020, 21, 7190.	4.1	7
95	Insight into conformational modification of alphaâ€synuclein in the presence of neuronal whole cells and of their isolated membranes. FEBS Letters, 2015, 589, 798-804.	2.8	6
96	Selective Targeting of αvβ5 Integrin in HepG2 Cell Line by RGDechi15D Peptide. Molecules, 2020, 25, 4298.	3.8	6
97	<i>fac</i> â€{Re(H <sub>2</sub> 0) <sub>3</sub> (CO) <sub>3</sub> ] <sup>+</sup> Complexed with Histidine and Imidazole in Aqueous Solution: Speciation, Affinity and Binding Features. ChemistrySelect, 2016, 1, 3739-3744.	1.5	5
98	Ubiquitin Associates with the Nâ€Terminal Domain of Nerve Growth Factor: The Role of Copper(II) Ions. Chemistry - A European Journal, 2016, 22, 17767-17775.	3.3	5
99	The change of conditions does not affect Ros87 downhill folding mechanism. Scientific Reports, 2020, 10, 21067.	3.3	5
100	Design, Optimization, and Structural Characterization of an Apoptosis-Inducing Factor Peptide Targeting Human Cyclophilin A to Inhibit Apoptosis Inducing Factor-Mediated Cell Death. Journal of Medicinal Chemistry, 2021, 64, 11445-11459.	6.4	5
101	Hemoprotein models based on a covalent helix-heme-helix sandwich 4. Discrimination of paramagnetic Fe(III)-Mimochrome I Δ and Λ isomers by NMR spectroscopy. Inorganica Chimica Acta, 1998, 278, 76-82.	2.4	4
102	Insight into the structural and functional features of myoglobin from Hystrix cristata L. and Rangifer tarandus L RSC Advances, 2015, 5, 26388-26401.	3.6	4
103	SPR and NMR characterization of the molecular interaction between A9 peptide and a model system of HER2 receptor: A fragment approach for selecting peptide structures specific for their target. Journal of Peptide Science, 2020, 26, e3231.	1.4	4
104	Metabolic and conformational stabilization of a VEGF-mimetic beta-hairpin peptide by click-chemistry. European Journal of Medicinal Chemistry, 2021, 222, 113575.	5.5	4
105	New synthetic tools for peptide-tetraphenylporphyrin derivatives. International Journal of Peptide Research and Therapeutics, 1998, 5, 269-276.	0.1	3
106	Structure and biological activity of a conformational constrained apolipoprotein A-I-derived helical peptide targeting the protein haptoglobin. RSC Advances, 2014, 4, 51353-51361.	3.6	3
107	Human Recombinant VEGFR2D4 Biochemical Characterization to Investigate Novel Anti-VEGFR2D4 Antibodies for Allosteric Targeting of VEGFR2. Molecular Biotechnology, 2019, 61, 513-520.	2.4	3
108	Probing the helical stability in a VEGF-mimetic peptide. Bioorganic Chemistry, 2021, 116, 105379.	4.1	3

**ROBERTO FATTORUSSO** 

#	Article	IF	CITATIONS
109	Biochemical and Conformational Characterization of Recombinant VEGFR2 Domain 7. Molecular Biotechnology, 2019, 61, 860-872.	2.4	2
110	Screening a Molecular Fragment Library to Modulate the PED/PEA15-Phospholipase D1 Interaction in Cellular Lysate Environments. ACS Chemical Biology, 2021, 16, 2798-2807.	3.4	2
111	Synthetic peptides mimicking the interleukin-6/gp 130 interaction: a two-helix bundle system. Design and conformational studies. Journal of Peptide Science, 2003, 9, 90-105.	1.4	1
112	Coordination of a bis-histidine-oligopeptide to Re( <scp>i</scp> ) and Ga( <scp>iii</scp> ) in aqueous solution. Dalton Transactions, 2019, 48, 15184-15191.	3.3	1
113	A novel approach for studying receptor-ligand interactions on living cells surface by using NUS/T1I•NMR methodologies combined with computational techniques: The RGDechi15D-αvβ5 integrin complex. Computational and Structural Biotechnology Journal, 2021, 19, 3303-3318.	4.1	1
114	Peptide-chelating agent conjugate for selective targeting of somatostatin receptor type 1: Synthesis and characterization. Biopolymers, 2004, 76, 527-534.	2.4	0
115	A New Ligand for Immunoglobulin G Subdomains by Screening of a Synthetic Peptide Library. ChemBioChem, 2005, 6, 1307-1307.	2.6	Ο
116	Structural characterization of the thermal unfolding pathway of human VEGFR1 D2 domain. FEBS Journal, 2022, 289, 1591-1602.	4.7	0
117	Design and synthesis of a porphyrin-linked cholecystokinin analog (CCK-9) as a diagnostic radiopharmaceutical. Nuclear Medicine Communications, 2000, 21, 587.	1.1	Ο
118	A second polymorph of a helical decapeptide. Peptide Research, 1994, 7, 55-9.	0.2	0
119	Modulation of the 20S Proteasome Activity by Porphyrin Derivatives Is Steered through Their Charge Distribution. Biomolecules, 2022, 12, 741.	4.0	0